Researches in Earth Sciences

Journal homepage: https://esrj.sbu.ac.ir

Research Article

Comparative assessing the performance of ANN, RF and CNN machine learning methods in identifying landslide prone areas

Sayyad Asghari Saraskanroud[1*], Maryam Riahinia[2], Batool Zeinali[3], Raoof Mostafazadeh[4]

1-Department of Physical Geography, Faculty of Social Science, University of Mohaghegh Ardabili, Ardabil, Iran

2-Department of RS & GIS, Faculty of Earth Sciences, Shahid Chamran University of Ahvaz , Ahvaz, Iran

3-Department of Climatology, Faculty of Social Sciences, University of Mohaghegh Ardabili, Ardabil, Iran

4-Department of Natural Resources, Faculty of Agriculture and Natural Resources, Water Management Research Center, University of Mohaghegh Ardabili, Ardabil, Iran

Received: 25 Jun 2025 Accepted: 30 Jul 2025

Abstract

Landslides are one of the natural hazards in mountainous areas that cause a lot of damage every year, thus, determining the landslide prone area is very important. This study assessed the performance of artificial neural network (ANN), Random Forest (RF), and Convolutional Neural Network (CNN) methods in identifying landslide prone areas. The study area is Lorestan Province, Khorramabad Watershed in western Iran, a region highly susceptible to landslides. After pre-processing the satellite images, the training samples were collected using field visits. Then, the neural network with a modifed structure was used for classification based on the simultaneous integration of the algorithm used. The available data were divided into 70% for the training, and 30 % for the validation stages. The performance of the generated classification maps of three employed methods were evaluated using the overall accuracy and confusion matrix. The results of evaluating the performance and accuracy of the CNN algorithm for identifying landslide areas show 93% overall accuracy. While the evaluation of the results obtained from ANN and RF methods shows that the overall accuracy of the neural network method is 90% and its overall accuracy is 88% and in the random forest method the overall accuracy is 84% and the overall accuracy is 82%; This study shows that the proposed method has shown the best performance compared to other methods according to evaluation criteria.These findings highlight the superiority of the CNN-based approach in accurately mapping landslide-prone areas, making it a reliable tool for future hazard assessment and risk management in mountainous regions.

Keywords: Landslide occurrence, Machine learning, Convolutional Neural Network, Landslide susceptibility mapping, Lorestan province.

Citation: Asghari Saraskanroud, S. et al, 2025. Comparative assessing the performance of ANN, RF and CNN machine learning methods, *Res. Earth. Sci:* 16(Special Issue), (73-91) DOI: 10.48308/esrj.2025.240455.1282

* Corresponding author E-mail address: s.asghari@uma.ac.ir

Introduction

Background

Landslides are among the most serious geological hazards worldwide, causing significant social, economic, and environmental damage, especially in mountainous regions, and influencing landscape evolution (Sun et al, 2021; Bragagnolo et al, 2020a; Pham et al, 2018; Merghadi et al, 2020). Between 2004 and 2016, landslides caused nearly 56,000 deaths globally (Froude and Petley, 2018), with recent events in Asia-Pacific and China causing major losses (Wang et al, 2020). Triggered by natural and human factors such as earthquakes, rainfall, deforestation, and land use changes, landslides disrupt infrastructure and urban development (Dou et al, 2019). Their impacts have worsened due to climate change and population growth, highlighting the need for effective risk management, with landslide susceptibility mapping (LSM) being a key tool for hazard mitigation (Ghorbani et al, 2023). Landslide susceptibility mapping (LSM) methods are generally classified into qualitative and quantitative categories. Qualitative approaches, which rely heavily on expert opinion, often suffer from subjectivity and demand considerable time and resources challenges that are particularly significant in developing regions. On the other hand, quantitative approaches apply statistical, probabilistic, and data-driven techniques (Tsangaratos et al, 2017; Aghayary et al, 2024), encompassing physically-based models, heuristic methods, and various machine learning (ML) algorithms. Among traditional ML techniques, random forests (RF), support vector machines (SVM), and multilayer perceptrons (MLP) have been widely used for LSM tasks (Martinović et al, 2016). With recent progress in GPU computing, deep neural networks (DNNs) have emerged as powerful tools for processing remote sensing data and mining spatial patterns (Mazzia et al, 2019; Esfandyari et al, 2024). Within this context, convolutional neural networks (CNNs) (a subset of DNNs) have attracted growing attention due to their capacity to automatically extract hierarchical spatial features. This makes them particularly effective for image-based applications such as landslide susceptibility mapping (Qi et al, 2019), which is the focus of the present study aiming to leverage this strength. In contrast to conventional machine learning approaches, convolutional neural networks (CNNs) are particularly effective in recognizing spatial patterns and local dependencies within data, thanks to their convolutional structure. This characteristic makes them highly suitable for image-driven applications such as landslide susceptibility mapping (Qi et al, 2019; Mazzia et al, 2019), whereas models like support vector machines (SVM) and multilayer perceptrons (MLP) often lack this spatial feature extraction capability.

Literature review

Zali and Shahedi (2021) assessed landslide sensitivity in the Neka Watershed, Mazandaran Province, using fuzzy logic combined with GIS. They integrated nine factors like slope, geology, and rainfall to create a landslide susceptibility map. Their findings showed that areas with steep slopes and low vegetation, especially sub-watersheds N2 and N1, had the highest landslide risk. Mohammadi and Sasanpour (2021) studied landslide susceptibility along the Haraz and Lavasanat roads in Tehran using GIS and spatial analysis. They analyzed factors like slope, rainfall, and faults to identify high-risk areas. Their results showed slopes over 50% and convex hillslopes near roads are especially vulnerable to landslides and debris flows. Rostamizad and Dastranj (2023) used SVM and 81 landslide sites to map landslide sensitivity in Chesb Watershed, Zanjan. They found 18.5% of the area at very high risk, with an AUC of 0.874 indicating strong prediction. Sharma et al. (2024a) created a high-resolution landslide map for India using ensemble learning and big geospatial data. Their model, combining ANN, RF, and SVM, tackled data imbalance and identified 4.75% of India as highly susceptible, including new risk zones in the Eastern Ghats. Agboola et al (2024) assessed landslide susceptibility in Polk County, North Carolina, using five machine learning models and two sampling scenarios. They aimed to optimize model accuracy through different non-landslide data selection methods and ensemble techniques. Their weighted average ensemble approach achieved up to 99.4% AUC-ROC, highlighting the strong influence of sampling strategy on model performance. Ali et al. (2024) conducted landslide susceptibility mapping in Northern Pakistan using both baseline and ensemble machine learning models. They identified slope, aspect, and

rainfall as key influencing factors. Among the models tested, logistic regression and XGBoost performed best, with XGBoost achieving an AUC of 0.907. The study underscores the value of ensemble approaches for improving landslide hazard prediction. Chicas et al (2024) reviewed global landslide susceptibility studies from 2001 to 2021, finding slope, elevation, lithology, land use, and road distance as key predictors. Random Forest was the most accurate model, while ANN showed stable performance.They called for more research in underrepresented areas like Africa and Central America. Bostan (2024) created a landslide susceptibility map for Kentucky, USA, using machine learning optimized by the artificial bee colony algorithm. The ABC-SGB model performed best, with intense rainfall, fault distance, and slope as top factors, highlighting the strength of hybrid models for prediction. Bammou et al (2025) evaluated landslide susceptibility in Morocco's Tensift sub-catchment using seven machine learning models. XGBoost achieved the highest accuracy with a 93.41% AUC, proving especially effective for semi-arid regions. Lokesh et al (2025) studied landslide susceptibility in Wayanad, Kerala, using machine and deep learning on 298 landslide sites. Random Forest outperformed other models with 97% accuracy, highlighting the value of data-driven methods for hazard mapping. Few studies directly compare ANN, RF and CNN on the same landslide dataset. Our study fills this gap by evaluating these models under identical conditions, providing new insights into their relative performance. Recent studies highlight the effectiveness of machine learning and deep learning models such as Random Forest (RF), Artificial Neural Networks (ANN), and convolutional neural networks (CNN) for landslide susceptibility mapping using geospatial data. However, direct comparative analyses of ANN, RF, and CNN on the same datasets remain scarce. This gap limits a clear understanding of their relative strengths, accuracy, and computational efficiency under varying conditions. While existing research demonstrates the potential of ML in landslide susceptibility mapping, comprehensive comparisons across traditional and deep learning models using unified datasets remain underexplored. Addressing this gap is essential for guiding more informed model selection and improving landslide prediction and management.

Scope and objective

Lorestan province is highly prone to landslides due to its geology, including alternating hard and loose rock layers, active tectonics, and seismic activity. The study area, located in the Zagros belt, is also home to the Seymareh landslide, one of the largest rocky avalanches worldwide. The aim of this study is to comparatively assess the performance of advanced machine learning methods, specifically Artificial Neural Network (ANN), Random Forest (RF), and Convolutional Neural Network (CNN), for landslide susceptibility mapping using satellite imagery in western Iran. The objectives include reviewing common machine learning approaches applied in landslide studies, proposing a CNN-based deep learning model for improved classification of landslide-prone zones, and evaluating the predictive accuracy of these models using field-verified training data. Model performance was validated through accuracy metrics such as confusion matrices and logistic regression analysis. This study provides a comprehensive comparison of traditional and deep learning models, highlighting the superior predictive capability of the CNN method, which achieved the highest overall accuracy, thereby demonstrating its potential as a reliable tool for landslide hazard assessment and risk management.

Materials and Methods

Study area

The study area is the Khorramabad Watershed, a sub-basin of the Kashkan basin within the larger Karkheh basin, covering 1,613 km² (about 16% of Kashkan). It lies between 48°04'–48°46' E and 33°15'–33°52' N, bordered by several mountains and plains. Lorestan province is recognized as a landslide-prone region in the country due to its geological features, including lithology, tectonic activity, seismicity, and climatic conditions. For instance, the alternating layers of hard calcareous rock and loose Marl-Shale along the edges of large anticlines throughout the province have contributed to the instability of extensive natural slope areas. The heavy rains during 1997-98 triggered numerous reactivations of old landslides and the

formation of new ones in various parts of the province. Currently, 86 villages in Lorestan are exposed to landslide hazards, and over 83,000 hectares of forest lie within landslide-prone zones. Geologically, Lorestan lies within the Zagros geological belt and is globally known for the Seymareh landslide, one of the largest rocky avalanche events. The basin's elevation ranges from 1,174 m at its outlet to 2,800 m at its highest point, with a main river length of 49.7 km. Its mountainous terrain leads to a climate that varies with altitude, featuring cold conditions in highlands and temperate climates in valleys. Geologically, the area belongs to the folded Zagros zone from the Cenozoic era, characterized by gentle folds, anticlines, and synclines mainly composed of limestone, marl, and evaporitic layers from the second and third geological periods (Stöcklin, 1968; Alavi, 2007). The region's geology is dominated by anticline structures with no igneous or metamorphic activity, and recent alluvial sediments form the flat plains.

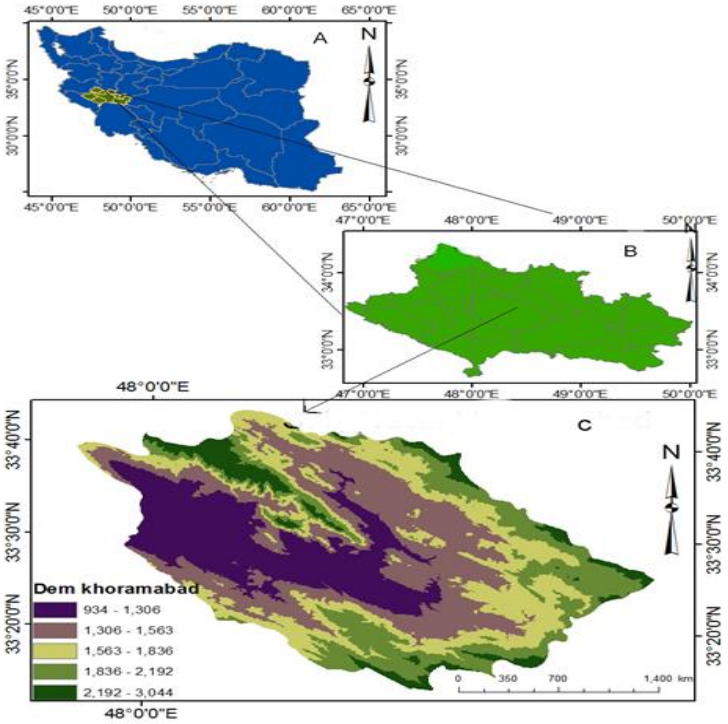

Fig. 1: Geographical location of the study area, A: Iran, B: Lorestan Province, C: Khorramabad watershed

Data set used

In this research, geological maps at the scale of 1: 100000 of the Geological Survey, topographic maps at the scale of 1: 50,000 of the geographical organization of the province, Landsat 8 satellite images of 2019, climatic data of the study area rainfall (2006 to 2019) From the Meteorological Organization of Lorestan Province, has been studied. DEM was used with a distance of 12.5 meters from the ALOS PALSAR satellite. The elevation was classified into five categories (Figure 2 a). Slope and aspect maps were also generated and classified into five and nine classes, respectively (Figures 2 b, 2 c). Rainfall data from 2006 to 2019 were analyzed using linear regression to develop a five-class rainfall map (Figure 2 d). In this process, both rainfall and elevation data were incorporated to establish a suitable regression model. After determining the regression equation, it was applied within the ArcGIS software environment, utilizing a Digital Elevation Model (DEM) as input. This approach enabled the accurate mapping of the spatial distribution of precipitation across the study area. The soil map, based on Lorestan province data, was divided into four classes (Figure 3 e). The soil map of Lorestan Province was classified into four classes based on the dominant soil types in the area (Figure 3 e). The classes include Inceptisols, Inceptisols/Vertisols, Rock Outcrops/Entisols, and Rock Outcrops/Inceptisols. Classification was based on soil properties, field observations, and the available soil map to accurately represent soil distribution in the area. Land use

was mapped using 2019 Landsat 8 images (30 m resolution), field surveys, and Google Earth, then classified into six categories using object-oriented methods in eCognition software (Figure 3 f). The distance maps from rivers and faults were generated by digitizing topographic and fault maps in ArcGIS. These maps were then classified into six categories for rivers and five categories for faults, respectively (Figures 3 g and 3 h). Finally, the lithological map was compiled from Geological Survey of Iran data at 1:100,000 scale and classified into six groups (Figure 3 I and Table 1).

Table 1: Detail of the classes of geological formations

Group	Geological Formation Details
1	River terraces and alluvial fans of old high and new low altitudes
2	Undifferentiated Bangestan Formation: limestone, shale, etc.; thick gray layer of orbitolin limestone, coral limestone, marl, dolomitic limestone, brown dolomite
3	Kashkan Formation (red conglomerate, sandstone, siltstone), Bakhtiari Formation (strongly cemented conglomerate), Bakhtiari conglomerate, marl
4	Aghajari Formation (grayish-brown limestone and sandstone), Fars Group (Gachsaran, Mishan), Amiran Formation, undivided Shahbazi and Asmari Formations, Tele Zang Formation, Radiolarite section, bituminous limestone, thick gray layer
5	Gurpi Formation (bluish-gray shale and marl containing argillaceous limestone), undifferentiated Eocene rocks, Gachsaran Formation (marl, sandstone, limestone), Asmari Formation

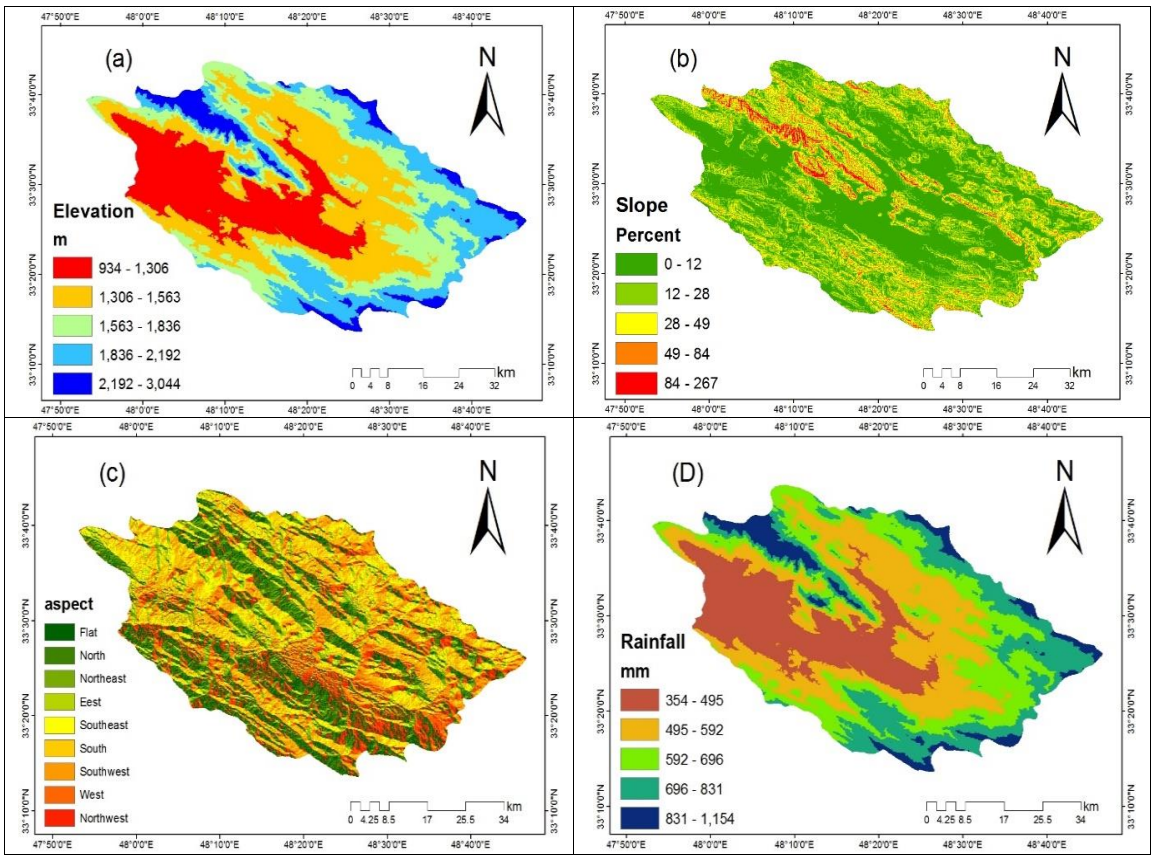

Fig. 2: The data layers used in this study, (a) elevation, (b) slope, (c) aspect, (d) Rainfall

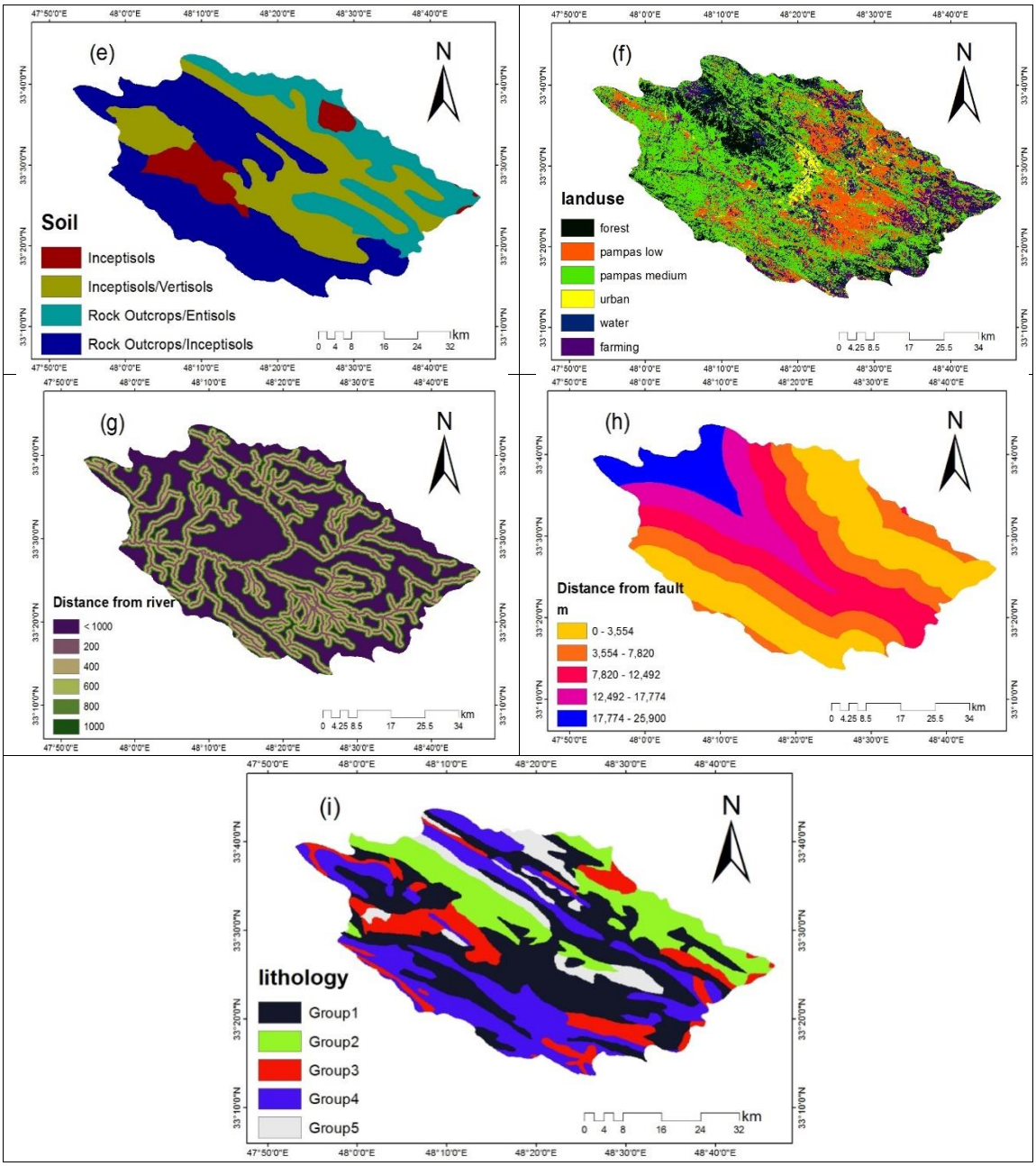

Fig. 3: The data layers used in this study, (e) soil, (f) land use, (g) distance from river, (h) distance from fault, (i) types of rocks

In this research, a binary classification approach was employed to differentiate between landslide and non-landslide zones. The dataset comprised 50 verified landslide occurrences and 70 randomly selected non-landslide locations, chosen to ensure spatial representation in regions without prior landslide activity. A total of 120 samples were utilized, with 70% assigned for model training and the remaining 30% reserved for testing.

Methodology

ArcGIS software was utilized to build the spatial database, conduct spatial analyses, and implement the final models (Asghari Saraskanrood et al, 2021; Asghari Saraskanrood and Piroozi, 2024). Geometric and radiometric corrections, as well as image processing, were carried out using eCognition and ENVI software. MATLAB 2013 was employed to develop the artificial neural network (ANN), random forest (RF), and deep neural network (DNN) models. SPSS software was used for evaluating and validating the models. Nine factors, including elevation, slope, slope aspect, land use, lithology, soil type, distance to faults, distance to rivers, and rainfall, were analyzed for landslide risk zoning using

ANN and RF models. Maps of these variables were prepared in ArcGIS and used as model inputs. The performance of the models was assessed and compared using logistic regression. The study began by reviewing existing literature to identify the key factors influencing landslide occurrence, followed by data collection and correction of satellite images and maps before analysis.

-Landslide Classification

Landslide-prone areas can be classified using three main approaches: pixel-based, object-based, and content-based methods. Recently, deep learning techniques have gained popularity for image classification due to their ability to utilize both spatial and temporal data content. These techniques can be applied in supervised or unsupervised modes. Given the higher accuracy of supervised methods in satellite image classification, this study adopts a supervised approach. The selected method is then compared with two widely used supervised classification techniques: the random forest algorithm and the perceptron neural network. A brief overview of the proposed algorithm and the comparative methods is provided next.

-Random forest (RF)

The Random Forest algorithm builds an ensemble of decision trees by repeatedly sampling the data and selecting random feature subsets for each tree, then combines their results through majority voting to make final predictions (Vorpahl et al, 2012). It excels in handling missing values and noisy data, providing robust and accurate outcomes with complex datasets (Zhou et al, 2021). Additionally, it captures nonlinear relationships and works with various data types without assuming normal distribution.

-Artificial Neural Network (ANN)

The artificial neural network (ANN), inspired by the human brain's structure, aims to replicate learning, generalization, and decision-making abilities (Lee et al, 2006). Its architecture, based on multilayer perceptrons, includes three main layers: the input layer for receiving environmental data; hidden layers that process inputs through weighted sums and activation functions to learn complex patterns; and the output layer that produces final results (Bragagnolo et al, 2020a). In multilayer networks, each hidden layer processes weighted outputs from the previous layer, with activation functions linking inputs to node values. ANNs can also model temporal dependencies by linking hidden layer nodes over time (Wang et al, 2020).

-Accuracy assessment

To assess and compare the performance of the applied methods and models, the root mean square error (RMSE), the correlation coefficient (R^2), and the mean absolute error (MAE) were employed (Sharma et al, 2024b). These statistical indicators, presented in Equations (1), (2), and (3), respectively, provide a quantitative basis for evaluating model accuracy and prediction performance (James et al, 2013).

Eq. 1)

$$\mathrm{RMSE} = \sqrt{\frac{1}{n}\sum_{i=1}^{n}(\mathrm{obs}_i - \mathrm{pre}_i)^2}$$

Eq. 2)

$$R^2 = \frac{\sum_{i=1}^{n}(\mathrm{obs}_i - \bar{y}_{\mathrm{obs}})(\mathrm{pre}_i - \bar{y}_{\mathrm{pre}})}{\sqrt{\sum_{i=1}^{n}(\mathrm{obs}_i - \bar{y}_{\mathrm{obs}})^2} \times \sqrt{\sum_{i=1}^{n}(\mathrm{pre}_i - \bar{y}_{\mathrm{pre}})^2}}$$

Eq. 3)

$$\mathrm{MAE} = \frac{1}{n}\sum_{i=1}^{n}|\mathrm{obs}_i - \mathrm{pre}_i|$$

Where, *obs* refers to the observed values, *pre* denotes the predicted values, and *N* represents the total number of data points used during the training and testing phases. In this study, nine factors were selected as input parameters, with a single neuron representing the output of the network. To assess the performance of the models in predicting landslide-prone areas, 50 known landslide locations within the study area were used for validation. It should be noted that the number of landslide data points used (50 points) represents the entire available dataset. However, efforts were made to select only those landslides with clear, reliable, and well-defined characteristics for training and evaluating the models, in order to maintain data quality and ensure scientifically valid and robust results. In this study, for binary modeling of landslide and non-landslide areas, 50 confirmed landslide samples and 70 randomly selected non-landslide samples (ensuring spatial distribution in areas with no landslide history) were used. These landslide/non-landslide samples were employed to train and validate the models (ANN and RF), enabling the models to effectively distinguish between landslide-prone and stable regions. A total of 120 data points were used, with 70% allocated for training and 30% for testing. In this study, the dataset was split into 70% for training and 30% for

validation, which is appropriate given the data volume and the research objectives. The simple train/test split allowed for easier interpretation and direct comparison of the models. This approach was sufficient and reasonable for the goal of the study, which was to evaluate and compare the models in identifying landslide-prone areas.

-Evaluation and validation of models by logistic regression method

In this study, logistic regression was used alongside the confusion matrix to provide deeper statistical insight into the classification models (artificial neural network and random forest) (Trigila et al, 2015; Hemasinghe et al, 2018). This method offers the ability to predict the probability of landslide occurrence, helps interpret the effect of each independent variable using regression coefficients and the Wald test, and evaluates model fit through indicators like Cox & Snell R^2, Nagelkerke R^2, and the Omnibus test. Its application strengthened the model's analytical depth and scientific credibility.LR models the relationship between a binary dependent variable (landslide presence/absence) and multiple independent variables, which can be continuous or discrete without requiring normal distributions. Unlike other methods requiring numerical or normally distributed variables, LR is flexible and can estimate odds ratios for each predictor, making it suitable for landslide sensitivity analysis.

Eq. 4)

$$p=\exp(z)/(1+\exp(z))$$

Where p is the probability of an event, here representing the likelihood of landslide occurrence, ranging from 0 to 1 in an S-shaped curve. The logistic regression fits the equation:

Eq. 5)

$$z=b0+b1x1+b2x2+\ldots+bnxn$$

Where z is a linear combination defined as z = b0 + b1x1 + b2x2 + ... + bnxn. Here, b0 is the intercept, bi are slope coefficients, and xi are the independent variables. This model relates landslide presence or absence to the predictor variables (Lee, 2005).

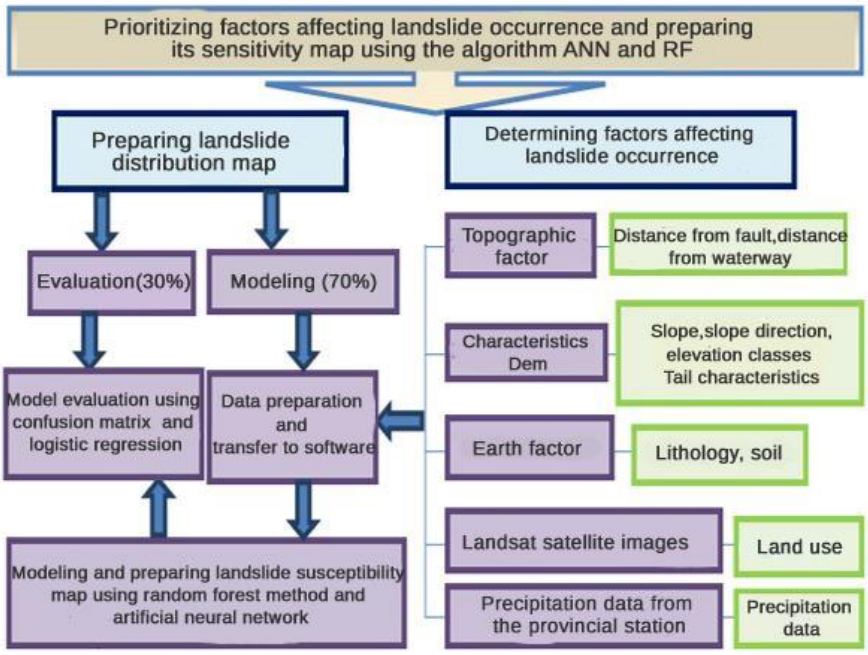

Fig. 4: Research method RF & ANN

-Convolutional Neural Network (CNN)

In recent years, deep learning has been widely used in data mining and remote sensing, especially for image classification due to its strong feature representation and automated learning capabilities (Li et al, 2024). Models like autoencoders can extract relevant features without traditional engineering. In remote sensing, 2D CNNs are popular for capturing spatial features from high-resolution images, which helps in object detection and segmentation (Wang et al, 2024). For crop classification, spatial 2D convolutions outperform 1D spectral methods by extracting both spatial and spectral information. CNNs, composed of multiple layers, learn hierarchical features from raw pixels, starting from spectral traits to complex patterns for object recognition (Alshehhi et al, 2017; Bouaafia et al, 2021). A typical CNN architecture (Figure 5) includes: 1)

convolutional layers that extract features, 2) pooling layers that reduce parameters and overfitting, and 3) fully connected layers for final classification. In this study, 20 multispectral Landsat 8 images from a specific geographic area were used to train and evaluate the designed model for landslide detection. These images, each containing 9 spectral bands, were selected from different months to capture seasonal, climatic, and surface cover variations. Due to the limited number of images, smaller fixed-size patches were extracted to increase the number of training samples. This approach not only expanded the dataset but also allowed for more precise local feature extraction by the network. All data were normalized before being input into the model and organized to be compatible with 3×3 3D convolutional kernels. Since the model focused on temporal changes within the same region, selecting data from a single area with high temporal diversity was scientifically justified and enhanced the model's accuracy in detecting landslide-related patterns in that region. The proposed model consists of two main parts: down-sampling and up-sampling, designed to extract spatial and temporal features from multispectral images. The down-sampling path includes six 3D convolutional layers, each using two 3×3×3 filters to jointly capture spatial and temporal information. MaxPooling layers with 2×2 filters are applied in the fourth and sixth layers to reduce dimensions and computational load, followed by ReLU activation. The up-sampling part includes three 3D convolutional layers aimed at reconstructing and enhancing extracted features for final decision-making. The number of filters in each layer was optimized through trial and error to achieve the highest evaluation accuracy. The model was trained using backpropagation with the Stochastic Gradient Descent (SGD) optimizer, a learning rate of $1e^{-3}$, batch size of 100, and 200 epochs. These settings were tuned based on model validation performance to achieve optimal results.

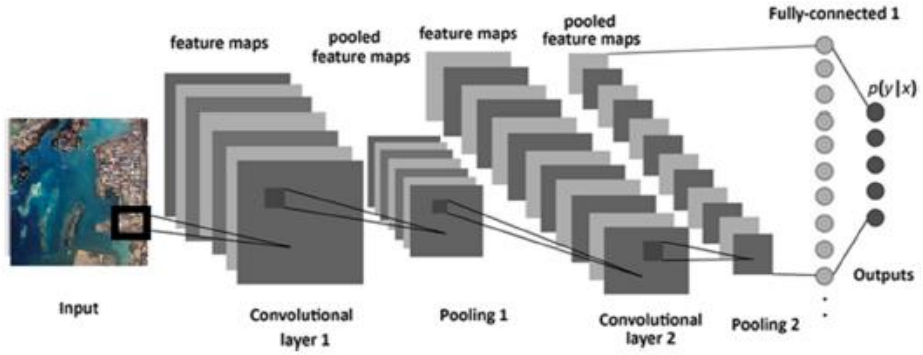

Fig. 5: The schematic of deep network architecture CNN, (Boulila et al, 2021)

Results and Discussion

To investigate the relationship between the factors affecting the occurrence of landslides in the desired area after preparing the distribution map of landslides ANN & RF, the distribution of these points to 9 factors affecting the occurrence of landslides in ArcGIS software environment was investigated Table 2.

Table 2: Key factors affecting landslides and shows the final landslide susceptibility map for Khorramabad Watershed.

Slope (Degree)	Ann	Class	0-12	12-28	28-49	49-87	87-267
		Landslide %	43.86	32.31	16.42	6.09	1.19
	RF		43.80	32.40	16.40	6.11	1.20
Soil	Ann	class	Inceptisols	Inceptisols/Vertisols	RockOutcrops/Entisols	RockOutcrops/Inceptisols	
	RF	Landslide %	8.47	31.80	20.18	40.47	
			8.42	31.75	20.18	40.52	
lithology	Ann	class	Group 1	Group 2	Group 3	Group 4	Group 5
		Landslide %	37.68	17.05	13.12	24.86	7.22
	RF		37.70	17.00	13.12	24.88	7.22
Distance from river(meter)	Ann	1000>	200	400	600	800	1000
		39.80	14.19	13.37	12.04	10.88	8.4
	RF	39.74	14.17	13.37	12.01	10.87	8.10
Landuse	Ann	Forest	pampas low	pampas medium	urban	Water	farming

		14.69	18.81	44.56	2.90	2.65	5.61		
	RF	14.72	18.79	44.50	2.84	2.60	5.51		
Distance from fault(meter)	Ann	class	0-3554	3554-7820	7820-12492	12492-17774	17774-25900		
		%	30.93	24.11	22.21	13.17	9.50		
	RF	%	30.90	24.11	22.15	3.15	9.47		
Rainfall (millimeter)	Ann	class	354-495	495-592	592-696	696-831	831-1154		
		%	21.95	29.04	23.38	18.63	6.56		
	RF	%	21.90	29.00	23.3	18.60	6.55		
Elevation(m)	Ann	Class	934-1306	1306-1563	1563-1836	1836-2192	2192-3044		
		%	21.91	26.41	23.27	18.71	5.07		
	RF	%	21.89	26.39	23.28	18.72	5.09		
Aspect	Ann	Flat	North	Northeast	East	Southeast	South	west	Southwest	Northwest
		6.79	13.16	6.10	12.10	12.65	15.32	3	12.72	10.31
	RF	6.75	13.11	6.9	12.07	12.62	15.30	3.86	12.70	10.30

Elevation: Elevation is a widely recognized factor in evaluating landslide susceptibility. In mountainous regions, external elements such as rainfall, vegetation, and human activities are closely linked to altitude, influencing landslide likelihood (Zhou et al, 2021). Generally, higher elevations are more prone to landslides. Neural network results show 16% of low-risk areas are between 934–1306 m, while 15% of high-risk areas are between 1836–2192 m. Random forest finds 17% low-risk in 934–1306 m and 25% high-risk in 1563–1836 m. This confirms landslide risk increases with elevation.

Slope: Slope affects surface and groundwater flow, impacting soil moisture and landslide initiation (Bragagnolo et al, 2020b). Landslides rarely occur on slopes less than 5° (Gomez and Kavzoglu, 2002). Neural network shows 32% of low-risk areas on 0–12° slopes, and 15% of high-risk on 12–28° slopes. Random forest results align with this. Landslides decrease on gentle slopes due to less gravitational force and on very steep slopes due to poor soil formation, making slope a critical factor.

Aspect: Aspect influences landslide susceptibility through exposure to wind and climate (Vorpahl et al, 2012), affecting weathering and moisture. Neural network shows low-risk mostly on southeast and south-facing slopes; high-risk on south and southwest slopes. Random forest shows similar trends, with high-risk also on flat slopes. North-facing slopes have higher humidity and vegetation, reducing landslides (Trigila et al, 2015). The highest landslide incidence is in south and southeast, so aspect matters but is not the main factor.

Land use: Land use affects landslide susceptibility as vegetation reduces soil erosion, runoff, and shallow landslides, aiding water absorption and evaporation (Trigila et al, 2015). Neural network shows 25% of low-risk areas in medium rangelands, also the highest for high-risk (20%). Random forest confirms this, with forest lands next in influence, likely due to their location in prone zones. Land use combined with other factors is important.

Rainfall: Rainfall saturates soil, increasing weight of unstable mass and affecting runoff (Wang et al, 2020; Sun et al, 2020). Neural network finds 19% low-risk areas with 354–495 mm rainfall; 11% high-risk with 592–696 mm. Random forest shows 20% low-risk and 33% high-risk in these ranges. Heavy rainfall often occurs at high altitudes and slopes with fewer landslides, so rainfall is important but interacts with other factors.

Distance from faults: Proximity to faults weakens rocks and soil, increasing landslide risk (Pham et al, 2018). Neural network shows 10–17% low-risk areas at 2,492–7,820 m from faults; 25% high-risk within 0–3,554 m. Random forest agrees. Landslide occurrence decreases with distance, making this an important factor (Zhou et al, 2021).

Distance to rivers: Distance to rivers influences landslides by affecting runoff and groundwater infiltration (Zhou et al, 2021). Neural network finds 18% low-risk and 22% high-risk within 1,000 m of rivers. Random forest shows similar results. Susceptibility decreases beyond 1,000 m, showing river proximity's significance.

Lithology: Lithology impacts landslides by affecting topography and rock strength (Wang et al, 2020). Areas with low permeability rocks have higher landslide potential (Zhou et al, 2021). Neural network shows 25% low-risk in river terraces/alluvial fans (group 1), and high-risk mostly in group 4 (Aghajari Formation,

Fars, Amiran). Random forest confirms this, making lithology a key factor.

Soil type: Soil type relates to geology and influences landslides (Mogaji et al, 2015). Neural network finds 25% low-risk in Inceptisol/Vertisol, and 10% high-risk in rock outcrop/Inceptisol. Random forest agrees, showing soil type's significant role.

To determine the landslide sensitivity index (LSI) for each class of factors, the probability ratio model was used due to its simplicity and high reliability (Lee et al, 2006). First, the frequency ratio was calculated, and then the landslide risk sensitivity index was computed using Eq 6 and 7 were applied to calculate the frequency ratio for each category of factors influencing landslide occurrence.

Eq. 6)

$$fr = \frac{Percentage\ of\ sliding\ pixels}{Percentage\ of\ non-slip\ pixels}$$

Eq. 7)

$$LSI = \sum fr$$

Where LSI is the Landslide Sensitivity Index for each category, and Fr is the frequency ratio of landslides in each category.

Landslide Sensitivity Mapping Using Neural Network and Random Forest

This study used a regular square grid method to divide all maps. After standardizing and layering the data, the information was imported into MATLAB for model analysis. Grid sizes ranged from 30 to 300 meters, with 100 meters chosen as optimal for the basin. The study area was divided into 251,634 pixels, each containing nine attribute values from the layers related to landslide factors. Two datasets of these digitized factors were then used for model analysis.

Map of landslide occurence

Using Landsat 8 satellite images, landslide occurrences and suspected prone areas were identified. Because many landslides are small or visually similar to surrounding slopes and thus hard to detect by satellite, field visits were conducted to verify landslides. A total of 50 landslide pixels were confirmed in the study area (Figure 6), with some landslide photos shown in Figure 7.

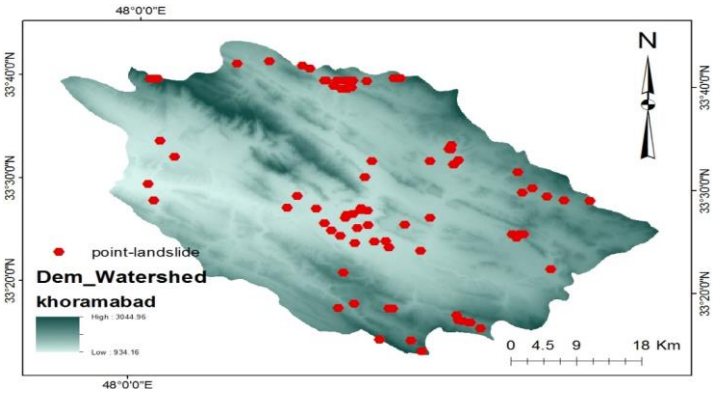

Fig. 6: Map of landslide and non-landslide points in Khorramabad Watershed

Fig. 7: Images of landslides in the study area

Landslide mapping using ANN

This study used a multilayer perceptron artificial neural network due to its superior performance and error propagation learning. Various network structures were tested, and the optimal one had 9 input neurons, 6 hidden neurons, and 1 output neuron (1-6-9). Landslide and non-landslide data (120 points) were

randomly split 70% for training and 30% for testing. The network achieved 92% overall accuracy in detecting landslide points. Each input neuron represented an effective landslide factor. After training, the network analyzed 251,634 pixels with 9 characteristics each, producing values between 0 and 1. These values were classified into five landslide sensitivity zones: very low, low, medium, high, and very high (Figure 8).

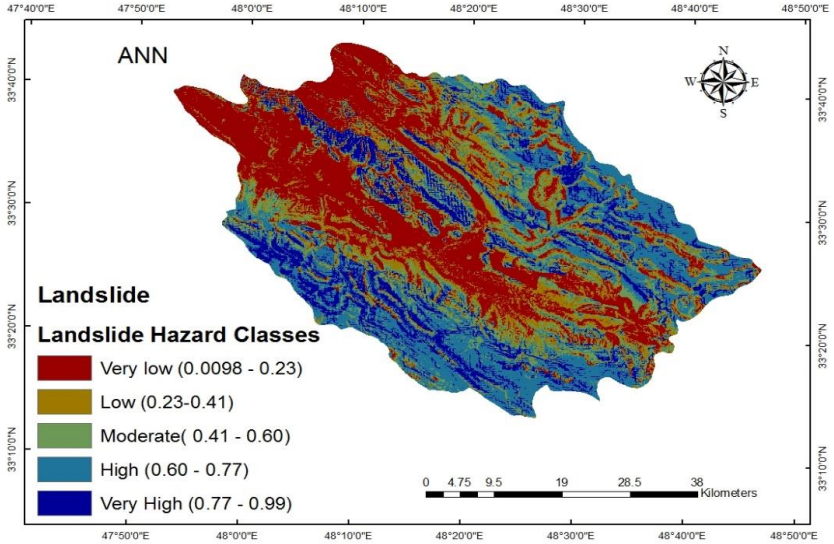

Fig. 8: Final map of landslide sensitive areas by artificial neural network method

Landslide mapping using Random forest model

The random forest model uses an ensemble of decision trees, averaging their results for classification. In this study, 9 landslide-related factors for 251,634 pixels were input into the model. Each pixel was classified based on majority voting from 3,000 trees with a leaf size of 5, determined by trial and error. Using 120 landslide and non-landslide points, data were split 70% for training and 30% for testing. The model correctly identified 43 out of 50 landslide cases, achieving 86% sensitivity. After minimizing error, the model classified the area into five susceptibility zones: very low, low, medium, high, and very high (Figure 9).

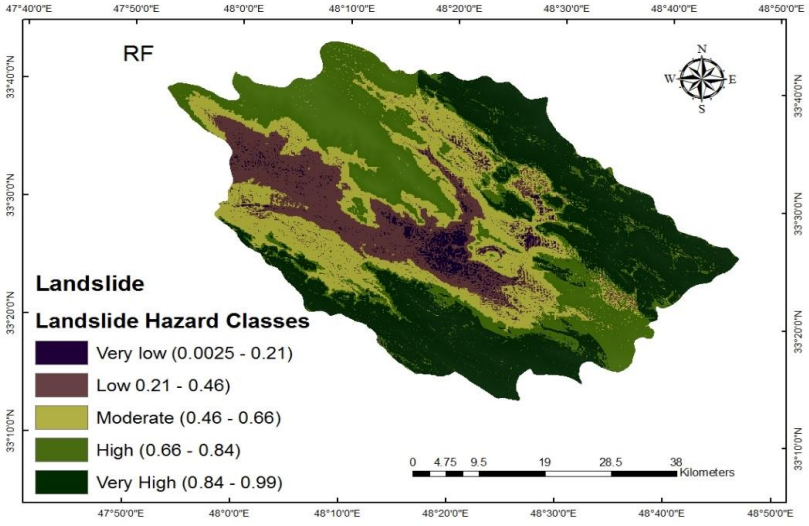

Fig. 9: Final map of landslide sensitive areas by random forest method method

To assess the overall landslide risk, the area of each sensitivity class was calculated. According to Table 3, the neural network model classified 13.36% of the area as very high risk and 25.27% as high risk. In contrast, the random forest model identified 33.36% as very high risk and 26.97% as high risk.

Table 3: Percentage of area with different potential in artificial neural network and random forest

Area	very little	Low	Medium	much	very much
ANN	31.18	16.08	14.09	25.27	13.36
RF	2.61	14.60	22.35	26.97	33.36

Landslide mapping accuracy and validation

Classifier validation results are often shown using confusion matrices, which display how observed classes compare to predicted classes. For binary classification, these matrices highlight true positives (TP), true negatives (TN), false positives (FP), and false negatives (FN) (Ruuska et al, 2018). To evaluate and compare the ANN and RF models, confusion matrices and accuracy metrics were used. The ANN achieved 90% overall accuracy, correctly identifying 92% of landslides and 88% of non-landslide areas, respectively (Figure 10 a). The RF model showed 84% overall accuracy, detecting 86% of landslides and 82% of non-landslide areas correctly (Figure 10, b). For identifying key factors in landslide occurrence, the RF model used the Mean Decrease Accuracy (MDA) index, highlighting slope, altitude, and rainfall as most influential, while land use, lithology, and distance to rivers had least impact. The ANN used connection weights (CW) to rank factors, showing slope, height, and distance from faults as most significant, with lithology, aspect, and land use as least impactful.

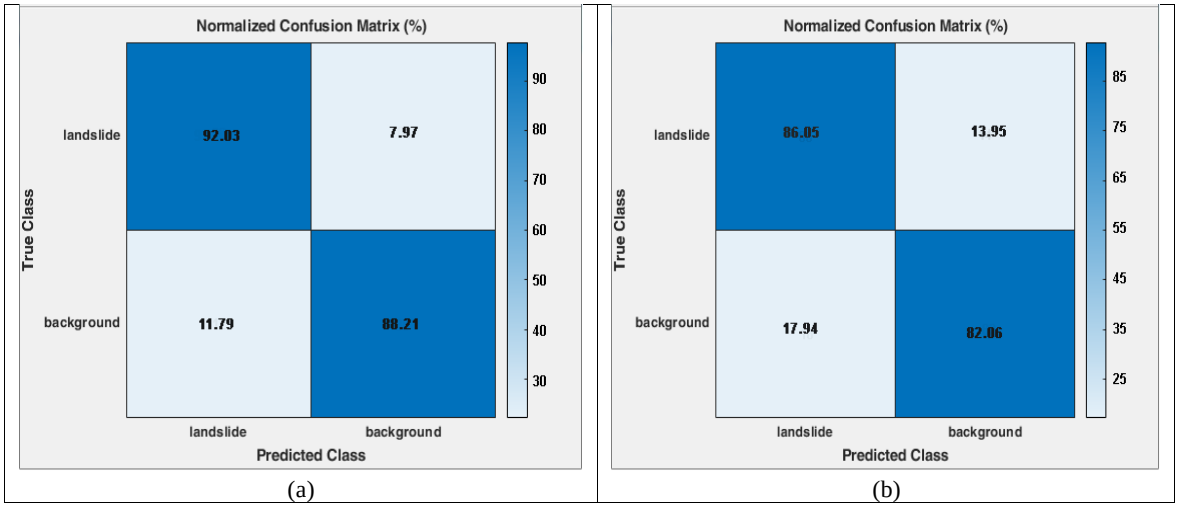

Fig. 10: a: Confusion matrix ANN, b: Confusion matrix RF

The overall significance of the models was tested using the Chi-square test, which assesses how well the model fits the data. Table 4 shows the test results: Chi-square values are 181,368.713 for the Random Forest model and 162,402.177 for the Artificial Neural Network model, both with p-values below 0.05. This indicates that both models fit well and that the independent variables effectively predict landslides.

Table 4: Omnibus Tests of Model Coefficients

		Chi-square	df	Sig.
Model	RF	181368.713	22	.000
	ANN	162402.177	22	.000

Each regression in the models has parent statistics with significance levels, similar to t-values in linear regression. Table 5 shows that in the ANN model, soil, distance from fault, distance from river, lithology, slope, and slope direction significantly affect landslides, while land use is not significant. The strongest effect is from distance from fault (Wald: 53175.235, $p < 0.05$), followed by slope and soil. Land use has the least effect (Wald: 2128.148, $p > 0.05$). In the RF model, soil, distance from fault, lithology, slope, slope direction, and precipitation are significant, but land use and distance from river are not. Precipitation has the greatest effect (Wald: 18646, $p < 0.05$), followed by soil and slope, while land use has the least effect (Wald: 1145.056, $p > 0.05$).

Table 5: Variables of the developed regression models

Model	Factors	B	S.E.	Wald	df	Sig.	Exp(B)
ANN	soil	-	-	14350.0	3	0.000	-
	slope	0.089	0.001	23179.2	1	0.000	1.094
	sazand	-	-	7946.5	4	0.000	-
	river	-	-	12639.1	5	0.000	-
	landuse	-	-	2128.1	6	0.496	-
	fault	0.000	0.000	53175.2	1	0.000	1.000
	rain	0.000	0.000	2151.4	1	0.046	1.000
	aspect	0.000	0.000	1058.5	1	0.000	1.002
RF	soil	-	-	11538.4	3	0.000	
	slope	0.144	0.002	7394.4	1	0.000	1.155
	sazand	-	-	631.3	4	0.000	-
	river	-	-	361.1	5	0.062	-
	landuse	-	-	1145.0	6	0.260	-
	fault	0.000	0.000	1844.9	1	0.000	1.000
	rain	0.034	0.000	18646.7	1	0.000	1.035
	aspect	0.000	0.000	9.6	1	0.002	1.000

According to table 5, The main table for interpreting the results shows the significance and impact of each independent variable on the dependent variable. B refers to the unstandardized regression coefficient, and S.E. is the standard error. Wald is the key statistic for testing the significance of each independent variable in the model and is equivalent to the t-statistic in linear regression. Exp(B) is the exponentiated coefficient used for interpretation, similar to the standardized regression coefficient in linear regression. The results indicate that in the ANN model, variables such as soil, distance to fault, distance to river, lithology, slope, and slope aspect significantly affect landslides, while land use is not significant. The strongest influence is from distance to fault (Wald: 53,175.235, $p < 0.05$), followed by slope and soil. Land use has the least impact (Wald: 2,128.148, $p > 0.05$). In the RF model, soil, distance to fault, lithology, slope, slope aspect, and rainfall are significant. However, land use and distance to river are not. Rainfall shows the highest impact (Wald: 18,646, $p < 0.05$), followed by soil and slope, while land use again has the lowest impact (Wald: 1,145.056, $p > 0.05$). Coefficients Cox & Snell R^2 and Nagelkerke R^2 in Table 6 approximate the determination coefficient (R^2) for logistic regression, showing how much variance in the dependent variable the independent variables explain. For the ANN model, values are 0.476 and 0.790, indicating 47–79% of variance explained. For the RF model, values are 0.514 and 0.686, meaning 51–68% of variance explained.

Table 6: Model Summary of the developed regression models

Step	-2 Log likelihood	Cox & Snell R Square	Nagelkerke R Square
ANN	69456.700	0.476	0.790
RF	166722.302	0.514	0.686

To assess the model's ability to classify landslide zones, Figures 11a and b) show that the random forest model achieved 85% overall accuracy. It correctly classified 83.2% of low-landslide pixels (98,960 correct, 20,000 misclassified) and 86.7% of high-landslide pixels (114,995 correct, 17,679 misclassified). The artificial neural network model had a higher overall accuracy of 94.8%, with 82.07% accuracy in low-landslide areas (36,001 correct, 7,547 misclassified) and 97.3% in high-landslide areas (202,438 correct, 5,648 misclassified).

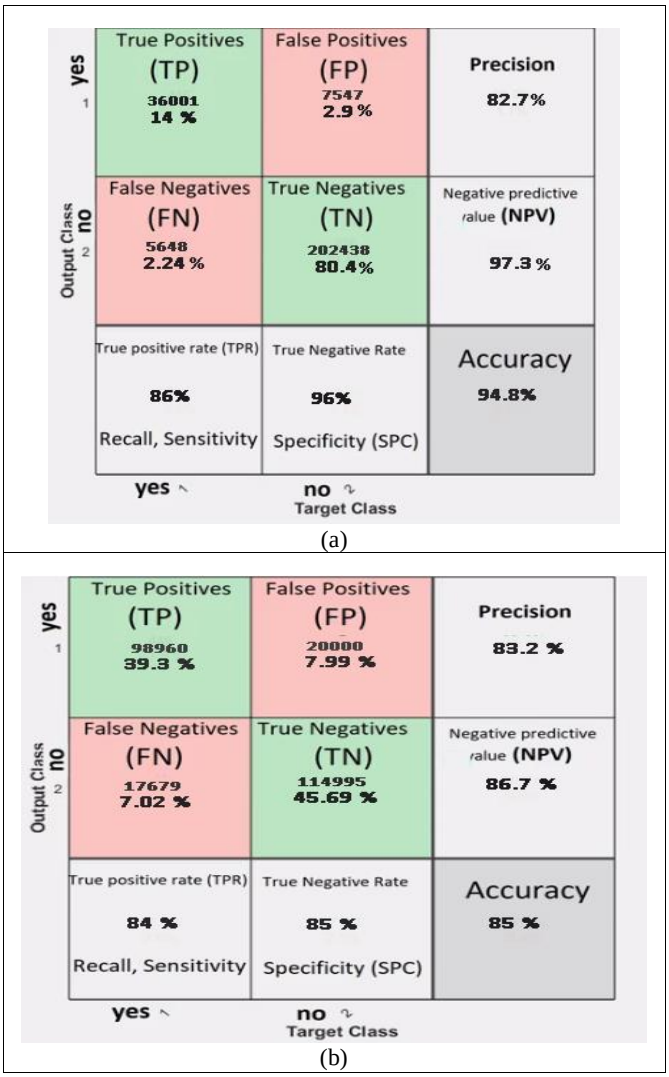

Fig. 11: Confusion matrix of a: ANN by logistic regression method, b: RF by logistic regression method

-Classification method based on deep learning using satellite images

Deep learning is an advanced image processing method well-suited for segmenting optical and partially obscured remote sensing images. It automatically extracts optimal features, handles complex problems, and processes large datasets like time series with low misclassification rates.

Data Preparation: This study used Landsat 8 OLI images with 9 spectral bands at 30m resolution, enhanced to 15m by PanSharpening in ENVI. Twenty images from before and after the 2018-2019 landslides were selected. Training samples were collected via GPS field visits, converted into polygons, and rasterized for classification. The same samples were used across algorithms for comparison.

Implementation: The CNN algorithm was used, requiring about 70% of field data for training and the rest for testing. Performance was evaluated quantitatively via confusion matrices. Processing ran on a 5-core Intel PC with 4GB RAM and 2GB graphics.

Network Architecture: The designed deep network has two parts: downsampling (6 layers, including 2 convolutional layers with 3×3 3D kernels) and upsampling (3 convolutional layers). Max pooling (2×2) was applied to reduce computation and improve training efficiency. Backpropagation with SGD optimizer and a learning rate of 1e-3 was used. The final output is a landslide prediction map (Figure 12).

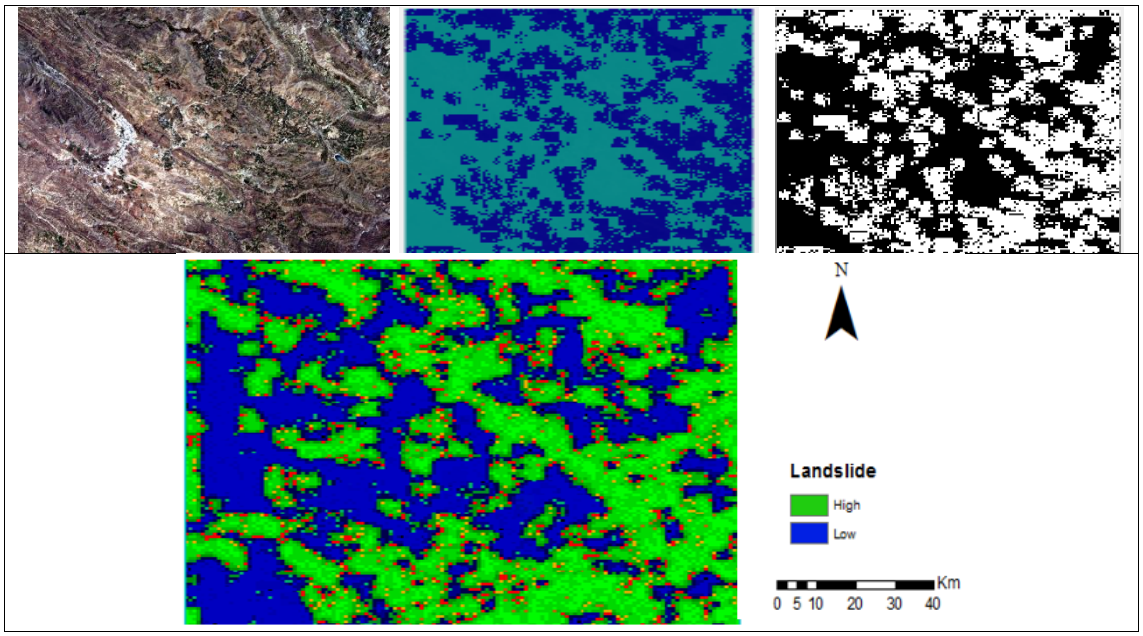

Fig. 12: The final classification map of the method CNN

The classification map's performance was evaluated using overall accuracy from the confusion matrix, which is the ratio of correctly classified pixels to total pixels. Diagonal elements show correctly classified pixels per class. User accuracy (row-based) and producer accuracy (column-based) were also calculated. Using 30% of data for evaluation, the model achieved 93% overall accuracy, with landslide and non-landslide classes correctly detected at 93% and 92%, respectively. Only 7% of pixels were misclassified as landslide, showing lower error and better accuracy than the ANN and RF models (Figure 13).

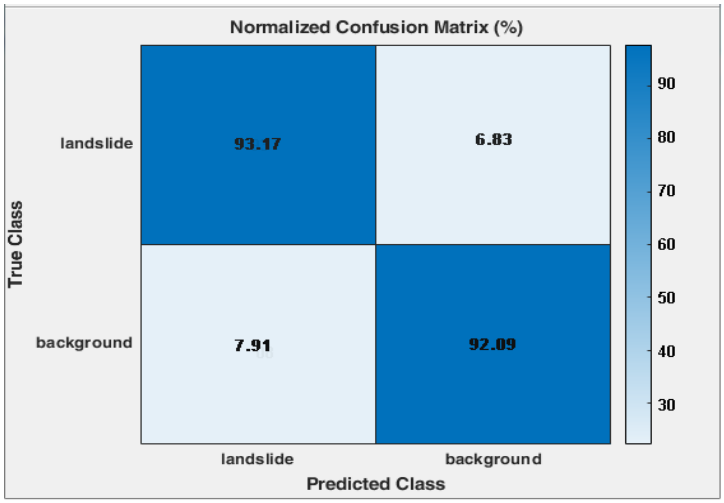

Fig. 13: Confusion matrix of CNN

Conclusion

This study compared the performance of artificial neural networks (ANN), random forest (RF), and a new deep learning method for landslide classification using satellite images. The ANN model identified about 47% of the area as low landslide risk and 38% as high risk, while RF showed 17% low and 50% high risk. Overall accuracy was 90% for ANN and 84% for RF, with ANN outperforming RF by about 6%. Logistic regression confirmed the significance of variables like distance from fault, slope, soil, and rainfall in predicting landslides. ANN achieved 94% overall accuracy, classifying 82% of low-risk and 97% of high-risk landslides correctly; RF had 85% overall accuracy. A novel deep learning model using a fully convolutional neural network (CNN) was designed, reducing training time while improving accuracy. The CNN achieved

93% overall accuracy, outperforming ANN by 3% and RF by 9%. CNN effectively captures temporal and spectral features of multi-temporal satellite images, offering more reliable classification results. Despite requiring large training datasets and challenges in generalization, CNN showed superior performance in landslide detection. Accurate landslide mapping is crucial for disaster prevention and mitigation by identifying high-risk areas early. Satellite imagery enables rapid detection of landslide-affected zones, aiding timely intervention. Future research may explore other neural network architectures like recurrent or capsule networks and develop hybrid deep learning models for enhanced landslide prediction.

Acknowledgment

The authors received no funding or financial support from any institution or organization related to this research.

References

Agboola, G., Beni, L.H., Elbayoumi, T. and Thompson, G., 2024. Optimizing landslide susceptibility mapping using machine learning and geospatial techniques. Ecological Informatics, v. 81, 102583. https://doi.org/10.1016/j.ecoinf.2024.102583

Aghayary, L., Asghari Saraskanrood, S. and Zeynali, B., 2024. Identification and zoning of landslide prone areas in Germi city. Journal of Hydrogeomorphology, v. 11(39), p. 1-18. https://doi.org/ 10.22034/hyd. 2024. 58703.1709 (In Persian).

Alavi, M., 2007. Structures of the Zagros fold-thrust belt in Iran. American Journal of science, v. 307(9), p. 1064-1095. http://dx.doi.org/10.2475/09.2007.02 (In Persian).

Ali, N., Chen, J., Fu, X., Ali, R., Hussain, M.A., Daud, H. and Altalbe, A., 2024. Integrating machine learning ensembles for landslide susceptibility mapping in Northern Pakistan. Remote Sensing, v. 16(6), 988 p. https://doi.org/10.3390/rs16060988

Alshehhi, R., Marpu, P.R., Woon, W.L. and Dalla Mura, M., 2017. Simultaneous extraction of roads and buildings in remote sensing imagery with convolutional neural networks. ISPRS Journal of Photogrammetry and Remote Sensing, v. 130, p. 139-149. https://doi.org/10.1016/j.isprsjprs.2017.05.002

Asghari Saraskanrood, S., Emami, R. and Piroozi, E., 2021. Evaluation and zonation of Landslide hazard with using OWA and ANN methods (case study: Paveh Township). Journal of Natural Environmental Hazards, v. 10(28), p. 131-150. 10.22111/jneh.2021.33729.1645 (In Persian).

Asghari Saraskanrood, S. and Piroozi, E., 2024. Identification and Zoning of Areas Prone to the Occurrence of Landslides Using the Aras Multi-Criteria Analysis Method (Study Area: Qaranqoochay Watershed in the Southeast of East Azarbaijan Province). Geography and Environmental Planning, v. 35(3), p. 65-94. 10.22108/gep.2024.140985.1639 (In Persian).

Bammou, Y., Benzougagh, B., Ouallali, A., Kader, S., Raougua, M. and Igmoullan, B., 2025. Improving landslide susceptibility mapping in semi-arid regions using machine learning and Geospatial techniques. DYSONA-Applied Science, v. 6(2), p. 269-290. 10.30493/das.2025.484839

Bostan, T., 2024. Generating a landslide susceptibility map using integrated meta-heuristic optimization and machine learning models. Sustainability, v. 16(21), 9396. https://doi.org/10.3390/su16219396

Bouaafia, S., Messaoud, S., Maraoui, A., Ammari, A.C., Khriji, L. and Machhout, M., 2021, March. Deep pre-trained models for computer vision applications: traffic sign recognition. In 2021 18th International Multi-Conference on Systems, Signals & Devices (SSD), p. 23-28. IEEE. DOI: 10.1109/ SSD52085. 2021.9429420

Bragagnolo, L., Da Silva, R.V. and Grzybowski, J.M.V., 2020a. Artificial neural network ensembles applied to the mapping of landslide susceptibility. Catena, v. 184, 104240. https://doi.org/10.1016/j.catena.2019.104240

Bragagnolo, L., da Silva, R.V. and Grzybowski, J.M.V., 2020b. Landslide susceptibility mapping with r. landslide: A free open-source GIS-integrated tool based on Artificial Neural Networks. Environmental Modelling & Software, v. 123, 104565. https://doi.org/10.1016/j.envsoft.2019.104565

Chicas, S.D., Li, H., Mizoue, N., Ota, T., Du, Y. and Somogyvári, M., 2024. Landslide susceptibility mapping core-base factors and models' performance variability: A systematic review. Natural Hazards, v. 1-21. 10.1007/s11069-024-06697-9

Dou, J., Yunus, A.P., Bui, D.T., Merghadi, A., Sahana, M., Zhu, Z. and Pham, B.T., 2019. Assessment of advanced random forest and decision tree algorithms for modeling rainfall-induced landslide susceptibility in the Izu-Oshima Volcanic Island, Japan. Science of the total environment, v. 662, p. 332-346. https://doi.org/10.1016/j.scitotenv.2019.01.221

Esfandyari Darabad, F., Rostami, G., Mostafazadeh, R. and Abedini, M., 2024. Spatial assessment and zoning of landslide risk in Zamkan watershed using support vector machine and logistic regression. Journal of

Hydrogeomorphology, v. 11(40), p. 123-102. 10.22034/hyd.2024.61467.1737 (In Persian).

Feng, Q., Niu, B., Chen, B., Ren, Y., Zhu, D., Yang, J. and Li, B., 2021. Mapping of plastic greenhouses and mulching films from very high resolution remote sensing imagery based on a dilated and non-local convolutional neural network. International Journal of Applied Earth Observation and Geoinformation, v. 102, 102441. https:// doi.org/ 10.1016/ j.jag. 2021.102441

Feng, L., Maosheng, Z., Mao, Y., Liu, H., Yang, Ch., Ying Dong and Yaser A., 2025. Nanehkaran, Convolutional neural network-based deep learning for landslide susceptibility mapping in the Bakhtegan watershed, Scientific Reports 15:13250 | 10.1038/s41598-025-96748-3

Froude, M.J. and Petley, D.N., 2018. Global fatal landslide occurrence from 2004 to 2016. Natural Hazards and Earth System Sciences, v. 18(8), p. 2161-2181. 10.5194/nhess-18-2161-2018

Ghorbani, A., Mostafazadeh, R., Zabihi, M. and Jafari Roodsari, M., 2023. GIS-based determining the landslide hotspot occurrence using Getis-Ord Index in Gharnaveh Watershed, Golestan Province. Journal of Hydrogeomorphology, v. 10(36), p. 1-18. 10.22034/hyd.2023.55449.1679 (In Persian).

Gomez, H. and Kavzoglu, T., 2005. Assessment of shallow landslide susceptibility using artificial neural networks in Jabonosa River Basin, Venezuela. Engineering Geology, v. 78(1-2), p. 11-27. https://doi.org/ 10.1016/ j.enggeo.2004.10.004

Hemasinghe, H., Rangali, R.S.S., Deshapriya, N.L. and Samarakoon, L., 2018. Landslide susceptibility mapping using logistic regression model (a case study in Badulla District, Sri Lanka). Procedia engineering, v. 212, p. 1046-1053. https://doi.org/10.1016/j.proeng. 2018.01.135

James, G., Witten, D., Hastie, T. and Tibshirani, R., 2013. An Introduction to Statistical Learning: with Applications in R (v. 103). Springer.

Lee, S., 2005. Application and cross-validation of spatial logistic multiple regression for landslide susceptibility analysis. Geosciences Journal, v. 9, p. 63-71. 10.1007/BF02910555

Lee, S., Ryu, J.H., Lee, M.J. and Won, J.S., 2006. The application of artificial neural networks to landslide susceptibility mapping at Janghung, Korea. Mathematical Geology, v. 38, p. 199-220. DOI: 10.1007/s11004-005-9012-x

Li, J., Cai, Y., Li, Q., Kou, M. and Zhang, T., 2024. A review of remote sensing image segmentation by deep learning methods. International Journal of Digital Earth, v. 17(1), 2328827. https://doi.org/10.1080/17538947.2024.2328827

Lokesh, P., Madhesh, C., Mathew, A. and Shekar, P.R., 2025. Machine learning and deep learning-based landslide susceptibility mapping using geospatial techniques in Wayanad, Kerala state, India. HydroResearch, v. 8, p. 113-126. https://doi.org/10.1016/ j.hydres. 2024.10.001

Martinović, K., Gavin, K. and Reale, C., 2016. Development of a landslide susceptibility assessment for a rail network. Engineering Geology, v. 215, p. 1-9. https://doi.org/10.1016/j.enggeo.2016.10.011

Mazzia, V., Khaliq, A. and Chiaberge, M., 2019. Improvement in land cover and crop classification based on temporal features learning from Sentinel-2 data using recurrent-convolutional neural network (R-CNN). Applied Sciences, v. 10(1), 238 p. https://doi.org/10.3390/app10010238

Merghadi, A., Yunus, A.P., Dou, J., Whiteley, J., ThaiPham, B., Bui, D.T. and Abderrahmane, B., 2020. Machine learning methods for landslide susceptibility studies: A comparative overview of algorithm performance. Earth-Science Reviews, v. 207, 103225. https://doi.org/10.1016/j.earscirev.2020.103225

Mogaji, K.A., Lim, H.S. and Abdullah, K., 2015. Regional prediction of groundwater potential mapping in a multifaceted geology terrain using GIS-based Dempster–Shafer model. Arabian Journal of Geosciences, v. 8, p. 3235-3258. 10.1007/s12517-014-1391-1

Mohammadi, N. and Sasanpour, F., 2021. Landslide and debris flow risk analysis in Haraz and Lavasanat roads. Water and Soil Management and Modelling, v. 1(4), p. 14-29. Doi: 10.22098/mmws.2021.9138.1023

Pham, B.T., Shirzadi, A., Bui, D.T., Prakash, I. and Dholakia, M.B., 2018. A hybrid machine learning ensemble approach based on a radial basis function neural network and rotation forest for landslide susceptibility modeling: A case study in the Himalayan area, India. International Journal of Sediment Research, v. 33(2), p. 157-170. https://doi.org/10.1016/j.ijsrc.2017.09.008

Qi, G., Wang, H., Haner, M., Weng, C., Chen, S. and Zhu, Z., 2019. Convolutional neural network based detection and judgement of environmental obstacle in vehicle operation. CAAI Transactions on Intelligence Technology, v. 4(2), p. 80-91. https://doi.org/10.1049/trit.2018.1045

Rostamizad, G. and Dastranj, A., 2024. Evaluating the sensitivity of the landslide event using the support vector machine algorithm. Water and Soil Management and Modelling, v. 4(4), p. 299-312. 10.22098/mmws.2023.13934.1379 (In Persian).

Ruuska, S., Hämäläinen, W., Kajava, S., Mughal, M., Matilainen, P. and Mononen, J., 2018. Evaluation of the confusion matrix method in the validation of an automated system for measuring

feeding behaviour of cattle. Behavioural processes, v. 148, p. 56-62. https://doi.org/10.1016/j.beproc.2018.01.004

Sharma, A., Sajjad, H., Rahaman, M.H., Saha, T.K. and Bhuyan, N., 2024b. Effectiveness of hybrid ensemble machine learning models for landslide susceptibility analysis: Evidence from Shimla district of North-west Indian Himalayan region. Journal of Mountain Science, v. 21(7), p. 2368-2393. 10.1007/s11629-024-8651-7

Sharma, N., Saharia, M. and Ramana, G.V., 2024a. High resolution landslide susceptibility mapping using ensemble machine learning and geospatial big data. Catena, v. 235, 107653. https://doi.org/10.1016/j.catena.2023.107653

Stöcklin, J., 1968. Structural history and tectonics of Iran: a review. AAPG bulletin, v. 52(7), p. 1229-1258. https://doi.org/10.1306/5D25C4A5-16C1-11D7-8645000102C1865D

Sun, D., Wen, H., Wang, D. and Xu, J., 2020. A random forest model of landslide susceptibility mapping based on hyperparameter optimization using Bayes algorithm Geomorphology, v. 362, 107201. https://doi.org/10.1016/j. geomorph. 2020. 107201

Sun, D., Xu, J., Wen, H. and Wang, D., 2021. Assessment of landslide susceptibility mapping based on Bayesian hyperparameter optimization: A comparison between logistic regression and random forest. Engineering Geology, v. 281, 105972. https://doi.org/10.1016/ j.enggeo. 2020.105972

Trigila, A., Iadanza, C., Esposito, C. and Scarascia-Mugnozza, G., 2015. Comparison of Logistic Regression and Random Forests techniques for shallow landslide susceptibility assessment in Giampilieri (NE Sicily, Italy). Geomorphology, v. 249, p. 119-136. https://doi.org/10.1016/j.geomorph.2015.06.001

Tsangaratos, P., Ilia, I., Hong, H., Chen, W. and Xu, C., 2017. Applying Information Theory and GIS-based quantitative methods to produce landslide susceptibility maps in Nancheng County, China. Landslides, v. 14, p. 1091-1111. 10.1007/s10346-016-0769-4

Vorpahl, P., Elsenbeer, H., Märker, M. and Schröder, B., 2012. How can statistical models help to determine driving factors of landslides? Ecological Modelling, v. 239, p. 27-39. https://doi.org/ 10.1016/ j.ecolmodel. 2011.12.007

Wang, L., Zhang, M., Gao, X. and Shi, W., 2024. Advances and challenges in deep learning-based change detection for remote sensing images: A review through various learning paradigms. Remote Sensing, v. 16(5), 804 p. https://doi.org/10.3390/rs16050804

Wang, Y., Fang, Z., Wang, M., Peng, L. and Hong, H., 2020. Comparative study of landslide susceptibility mapping with different recurrent neural networks. Computers & Geosciences, v. 138, 104445. https://doi.org/10.1016/j.cageo.2020.104445

Zali, M. and Shahedi, K., 2021. Landslide sensitivity assessment using fuzzy logic approach and GIS in Neka Watershed. Water and Soil Management and Modelling, v. 1(1), p. 67-80. Doi: 10.22098/mmws.2021.1183. 10.22098/mmws.2021.1183

Zhou, X., Wen, H., Zhang, Y., Xu, J. and Zhang, W., 2021. Landslide susceptibility mapping using hybrid random forest with GeoDetector and RFE for factor optimization. Geoscience Frontiers, v. 12(5), 101211. https://doi.org/10.1016/j.gsf.2021.101211